Analysis of x-ray diffraction patterns from microprocessor controlled apparatus

W.T.Davie
School of Physics, University of Bristol.
(Dated: February 3, 2023)

The aim of this paper is to explore x-ray diffraction and absorption patterns, highlighting the information they provide and to examine the limitations of modern x-ray equipment using a variety of experimental methods. Four key results were recorded: The lattice constants of NaCl and Si; 2.834 ± 0.006Å and 5.425 ± 0.009Å respectively, a value of the Rydberg constant; $13,468,900 \pm 618600\text{m}^{-1}$ and a value of Planck's constant; $6.30 \times 10^{-34} \pm 1.4 \times 10^{-35}\text{m}^2\text{kgs}^{-1}$. Through the analysis of such results it was found that throughout calculations, important elements of theory were unaccounted for.

INTRODUCTION

The core ideas and discoveries of solid state physics are used throughout an array of subjects, such as chemistry, material science, geology and engineering. X-ray diffraction was the spark that ignited the study of solid state physics, it was theorized by Prof. M. von Laue and was experimentally proven by W. Friedrich and P. Knipping [1]. The work was published in 1912, not long after the discovery of x-rays by W. Röntgen in 1895 [3]. The paper quickly captured the attention of W.H. Bragg, who took Laus' ideas and formulated a neat description of x-ray diffraction known as Braggs Law [2]. In 1913 and 1914, Bragg was joined by his son Lawrence and began analysing crystal structures by x-ray diffraction.

This paper will use Braggs Law and demonstrate the remarkable extent of what an x-ray diffraction pattern can tell you about the internal structure of a crystalline solid. In addition, arguably more significantly, analytical methods will show how accurately such small details can be measured with the help of modern equipment. The x-ray apparatus used is the 'Leybold x-ray apparatus' and is controlled entirely by a microprocessor. To test its limitations further and present some interesting applications and results from the x-ray apparatus, the paper contains the analysis of a further two experiments.

The first will look at x-ray absorption spectra and analyse specifically the location of absorption edges. A key idea used will be a liner relationship between atomic number Z and $\frac{1}{\sqrt{\lambda}}$, where λ is the wavelength at which an absorption edge arises. This relationship was derived by H. Moseley following Bragg's work in 1913 and 1914 [3].

The last segment will take measured wavelengths λ_{min} (where x-rays of maximum energy are produced) at a range of voltages V and use the Planck relation to explore exactly how accurately the apparatus performs.

THEORY

Braggs Law [1][3]

When an x-ray is reflected by the planes of a crystal structure, as shown by FIG. 1, the reflected rays from each plane will interfere. At a characteristic angle θ between the plane and incoming rays; constructive interference will occur. Braggs Law relates θ to distance between planes d and the wavelength of the x rays λ by:

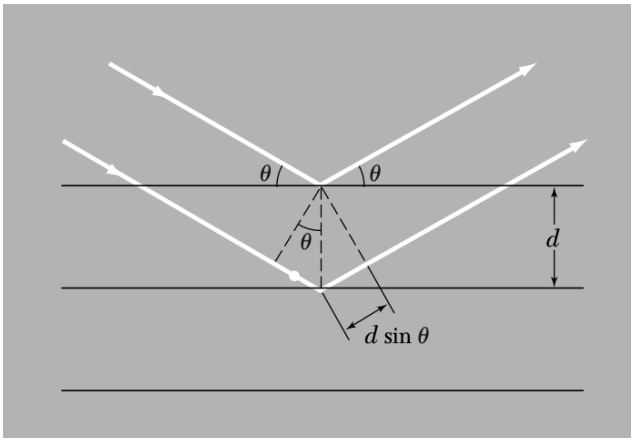

FIG. 1. A diagram showing three planes of a crystal structure and incoming x-rays. d is the lattice spacing and the labeled distance $d\sin\theta$ shows how Braggs Law is derived.

[1]

$$n\lambda = 2d\sin\theta \tag{1}$$

Where n is a positive integer.

It is possible to relate lattice spacing d to atom spacing or lattice constant a by:

$$d = \frac{a}{\sqrt{h^2+k^2+l^2}} \tag{2}$$

Where h, k and l are the Miller indices of a given plane. Miller indices were formulated by a mineralogist in the 19th century W. Miller. He found that the orientation of any plane within a crystal lattice can be described by three integers (hkl). Since the orientation of a plane has an indisputable effect on x-ray diffraction, miller indices appear throughout Laus' and Braggs work and hence this paper. Equation 2 can be derived from the Laue conditions (see Apendix).

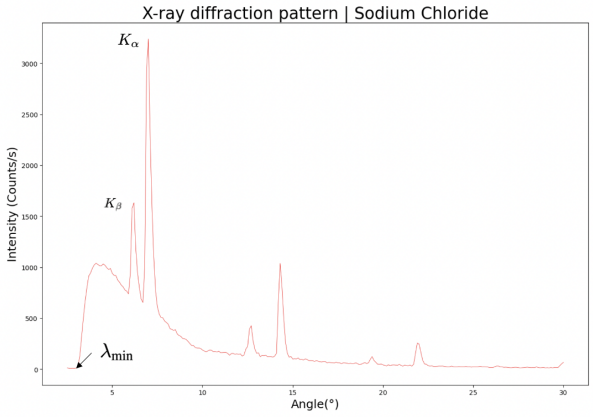

FIG. 2. A NaCl x-ray diffraction pattern measured by the Leybold x-ray apparatus. K_α and K_β indicate which wavelengths correspond to respective peaks of constructive interference. $\lambda_{\min}$ shows the angle at which incoming x-rays have the minimum wavelength.

Structure factor[4]

When a diffraction pattern is measured, such as the one shown by FIG. 2, the intensity of peaks varies. This has a direct connection to the orientation and location of the plane at which diffraction occurs, it's miller indices. The structure factor F_{hkl} is used to quantify the intensity I of a given peak. F_{hkl} can be described by:

$$F_{hkl} = \sum_{j=1}^{N} f_j e^{[-2\pi i(hx_j + ky_j + lz_j)]} \tag{3}$$

$$I = |F_{hkl}|^2 \tag{4}$$

f_j is known as the atomic form factor and corresponds to the amplitude of wave scattering by the j^{th} atom. Hence a summation across N atoms gives rise to an intensity.

Absorption Edges and Moseley's Law [3]

When x-rays are passed through a solid filter, in general, the lower the energy of incoming rays (higher wavelength λ), the more they are absorbed. However, when λ reaches a specific value, the x-rays no longer have the energy required to ionize an electron from inner, more stable, energy levels. As a result, a sudden drop in absorption occurs. The wavelength at which this 'absorption edge' appears is unique to each element and therefore can be related to atomic number Z. Mosley's Law describes this relationship:

$$\lambda^{-\frac{1}{2}} = R^{\frac{1}{2}}(Z - \sigma)^2 \tag{5}$$

Where R is the Rydberg constant and σ is the screening constant, which emerges due to the reduction of nuclear charge by other 'sheilding' electrons.

How X-rays are created[3][5]

Before X-rays are either absorbed or diffracted they must be created. There are two key ways in which x-rays are created. The first is known as 'Bremsstrahlung radiation'. X-rays are produced in this way when fast moving electrons are passed near a nucleus, the electrons experience a 'braking' effect and lose energy. The lost energy is carried away as EM radiation shown by:

$$\frac{hc}{\lambda} = E_1 - E_2 \tag{6}$$

Where h is plancks constant and c is the speed of light. Radiation created this way will have a range of wavelengths. The absolute maximum energy of x-rays produced will be when all electron energy is lost ($E_2 = 0$) and so:

$$\frac{hc}{\lambda_{\min}} = Ve \tag{7}$$

V is the voltage across an x-ray tube/electron accelerator. e is the charge of an electron. $\lambda_{\min}$ is therefore the minimum wavelength of produced x-rays and can be measured from a diffraction pattern shown in FIG. 2. Bremsstrahlung radiation produces a continuous distribution of intensity which can be described by Kramers' law:

$$I(\lambda)d\lambda = K(\frac{\lambda}{\lambda_{\min}} - 1)\frac{1}{\lambda^2}d\lambda \tag{8}$$

Where K can be described by:

$$K = 4\lambda_{\min} I_{\max}$$

The second way x-rays are created is also due to incoming, high energy electrons. In this case, the incoming electrons collide with inner energy level electrons within the tungsten anode of a x-ray tube. These electrons are ejected and hence provide a vacancy for electrons in outer energy levels. This paper concerns radiation as a result of two different electron transitions; K_α and K_β Shown by FIG. 3.

EXPERIMENTAL DETAILS

Using the Leybold x-ray apparatus is a relatively simple process. In order to obtain the diffraction patterns for NaCl and Si, the following settings were used: Tube voltage: $35kV$, Current: $1mA$, Time between readings(Δt): $1s$, Change in angle($\Delta\theta$): $0.1°$. Once the apparatus is set, a sample of the required solid is placed onto a target. Followed by a simple click of a button measurements begin, the results are displayed on a connected desktop.

To collect attenuation spectra data, caps are placed onto the x-ray source. Before doing so, a 100% transmission spectra

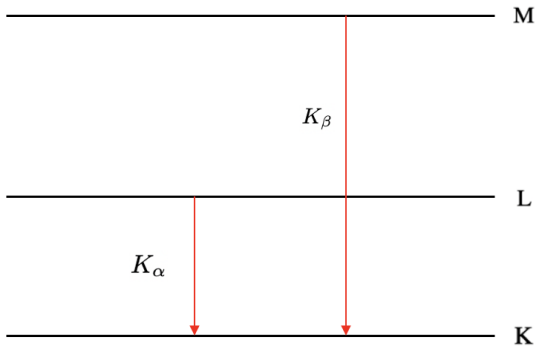

FIG. 3. An energy level diagram containing three electron energy states, K L and M. When an electron transitions from L to K, K_α radiation is emitted. Similarly from M to K, K_β raditation is emitted

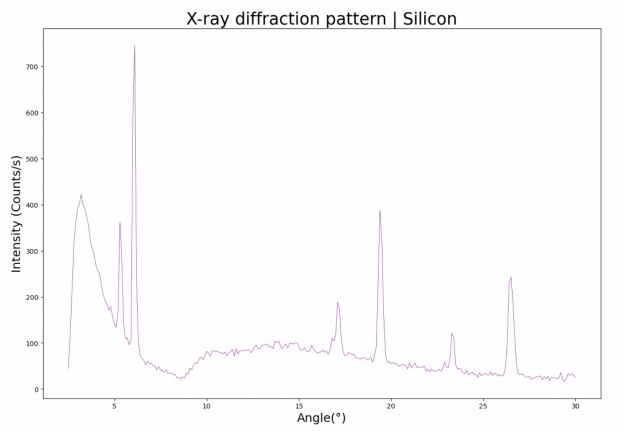

FIG. 4. A Si x-ray diffraction pattern measured by the Leybold x-ray apparatus.

is first recorded. In this case, using the same settings, spectra for five different elements was measured; Ag, Zr, In, Nb, Mo.

Lastly, by placing NaCl back onto the target and altering tube voltage in steps of $2.5kV$ over the range $20kV - 35kV$ a range of λ_{min} values was acquired (equation 7).

RESULTS AND ANALYTICAL METHODS

Diffraction

A total of six diffraction patterns were recorded, three for sodium chloride (NaCl) and three for Silicon (Si). The 'average pattern' for NaCl and Si is shown by FIG. 2 and 4 respectively. Each figure shows sharp peaks of intensity as Bragg's law predicts, Furthermore, in conjunction with the theory of how x-rays are created, pairs of peaks arise. Where the first pair emerge when $n = 1$, the second at $n = 2$ and so on. However, Bragg's Law does not predict the broad peaks observed. In every case the width of the peaks appears almost

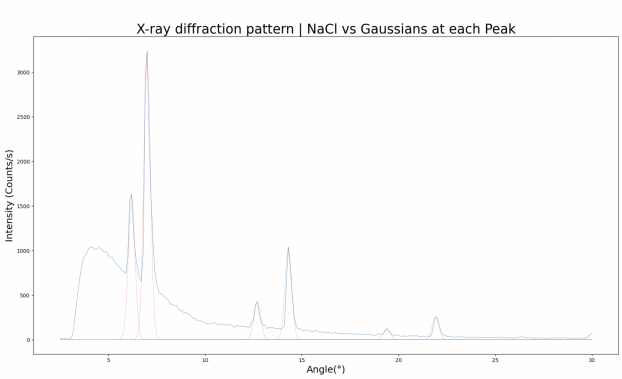

FIG. 5. A NaCl x-ray diffraction pattern measured by the Leybold x-ray apparatus. Along side this pattern are Gaussian distributions where the mean is the angle of max intensity and the FWHM is given $4\Delta\theta$.

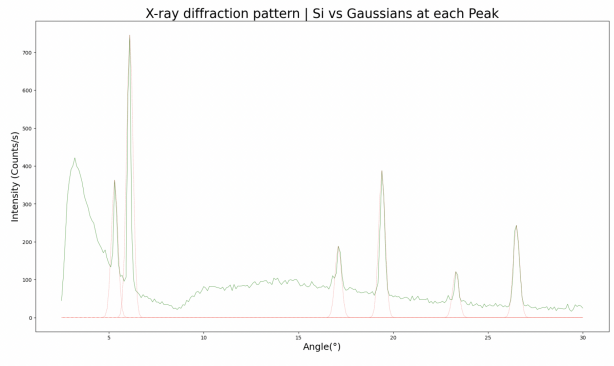

FIG. 6. A Si x-ray diffraction pattern measured by the Leybold x-ray apparatus. Along side this pattern are Gaussian distributions where the mean is the angle of max intensity and the FWHM is given $4\Delta\theta$.

exactly equivalent. This can be shown by the convolution of a Dirac-delta function at each peak with a gaussian. i.e.

$$f_i(\theta) = \delta(\theta - \theta_i)$$

$$g_i(\theta) = I_i e^{-\frac{\theta^2}{2\sigma^2}}$$

$$h_i = f_i * g_i$$

Where θ_i and I_i are the angle and max intensity of the i^{th} peak. $h_i(\theta)$ has been plotted for each peak and is displayed alongside each diffraction pattern in FIG. 5 and FIG. 6. What is interesting and important to note is that for each gaussian standard deviation σ is equal for each peak yet very closely represents the observed pattern. The σ used is identical to $\frac{4\Delta\theta}{2.355}$ and was predicted by taking an average full width half maximum. Early Si peaks ($n = 1$) do not follow their given distribution perfectly, presenting areas of investigation.

Prior to calculating a lattice spacing for each pattern, by taking the literature value of lattice spacing for NaCl and Si

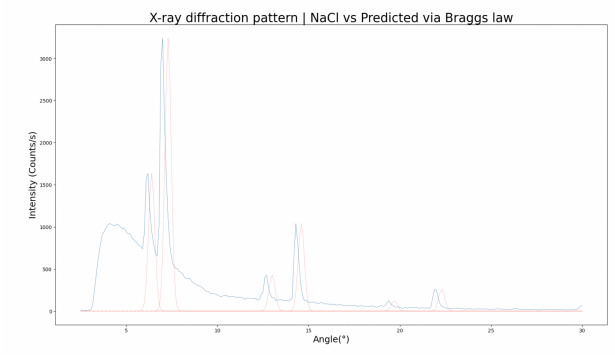

FIG. 7. A NaCl x-ray diffraction pattern measured by the Leybold x-ray apparatus. Along side this pattern are Gaussian distributions where the mean is the angle of max intensity predicted by Bragg's law and the FWHM is given $4\Delta\theta$.

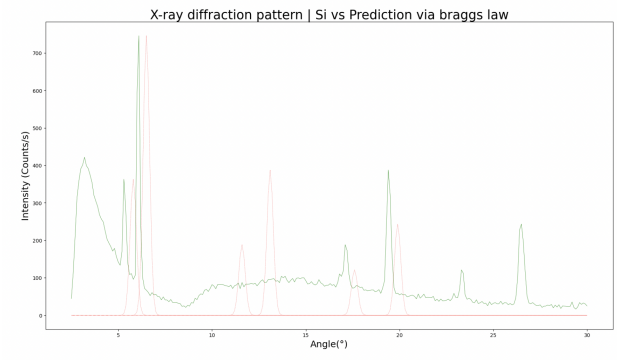

FIG. 8. A Si x-ray diffraction pattern measured by the Leybold x-ray apparatus. Along side this pattern are Gaussian distributions where the mean is the angle of max intensity predicted by Bragg's Law and the FWHM is given $4\Delta\theta$.

and applying equation 1, both FIG. 7 and 8 are produced. Note that the same standard deviation as previous has been applied. The difference between predicted peaks and experimental results for NaCl was a constant value of $0.30°$. It seems that the diffraction pattern has been 'shifted'. For Si, the major observation here is that Braggs law predicts the existence of peaks that are not present experimentally. This observation can be proven mathematically by solving equation 3. However, we do also see a 'shift' for correctly predicted peaks in this case slightly larger at $0.45°$. Taking the location of each peak measured experimentally followed by applying the standard deviation previously stated as the error. Braggs law can again be used to calculate a lattice spacing d. The results were $d_{\text{NaCl}} = 2.834 \pm 0.006$Å and $d_{\text{Si}} = 3.132 \pm 0.005$Å.

The other striking result is the underlying continuous intensity spectrum that rises initially and then descents to an asymptote at 0. This is a result of Bremmstrahlung production of x-rays and by using Kramers' Law (8) a similar shape can be plotted against the results. See FIG. 9.

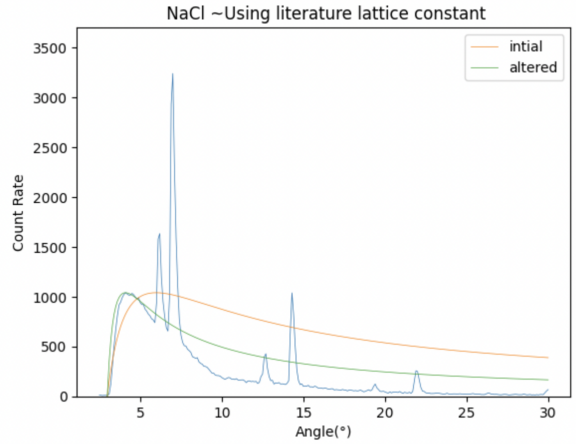

FIG. 9. A plot of Kramer's law alongside an NaCl diffraction pattern. The first 'inital' plot uses parameters give by the the pattern, the second 'altered' plot uses Kramers Law with tweaked parameters.

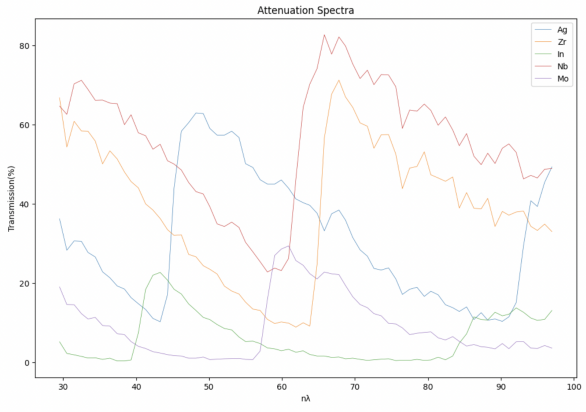

FIG. 10. Absorption spectra for a range of elements, measured by the Leybold x-ray apparatus.

Absorption edges

The attenuation spectra for all measured elements is displayed by FIG. 10. All spectra have at least one absorption edge. The analysis of each edge is relatively simple and can be visualized by FIG. 11. Values $n\lambda$ at minimum and maximum transmission are recorded, the mid point provides a mean result and half the difference gives the error. By applying Moseley's law (5) using known values of Z and recorded values of $n\lambda$ a linear plot can be fitted, see FIG. 12. The gradient of this linear fit corresponds $R^{1/2}$ (see equation 5). The rydberg constant obtained was $13,468,900 \pm 618600\text{m}^-1$

Determining Planck's constant

Looking back at FIG. 2 and equation 7, it is possible to measure values of λ_{min} from a diffraction pattern. Since the

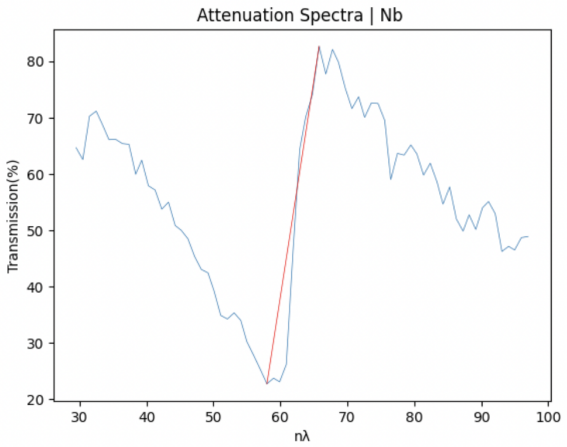

FIG. 11. A measured Nb absorption spectra fitted with a red line to indicate the difference between the minimum and maximum transmission

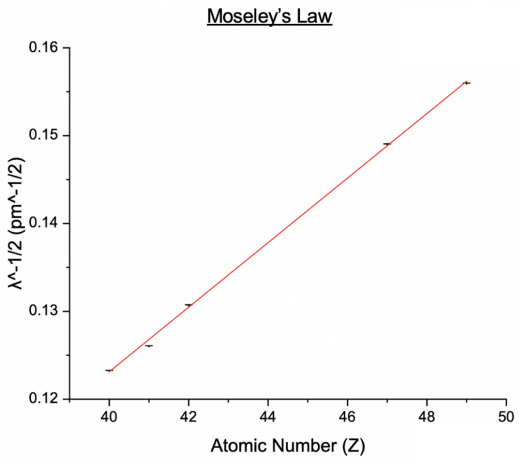

FIG. 12. A linear fit of Moseleys law using measured values of λ for five elements.

voltage across the x-ray tube is known and can be changed using a dial on the Leybold apparatus, a linear relationship between voltage and $\frac{1}{\lambda_{\min}}$ can be plotted. The range of diffraction patterns observed and the linear fit are shown by FIG 13 and 14 respectively. The gradient of FIG. 14 is Planck's constant. The result was $6.30 \times 10^{-34} \pm 1.4 \times 10^{-35} \mathrm{m^2 kgs^{-1}}$

DISCUSSION

The primary goal of this discussion is to compare how the experimental diffraction and attenuation patterns stray away from what the theory predicts and hence understand the limitations of the apparatus.

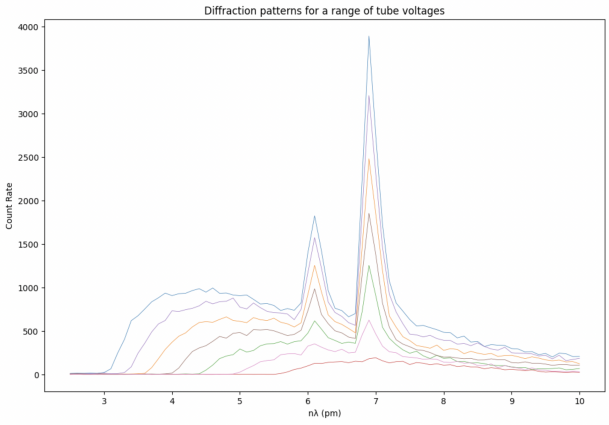

FIG. 13. Multiple NaCl diffraction patterns each recorded at different tube voltages.

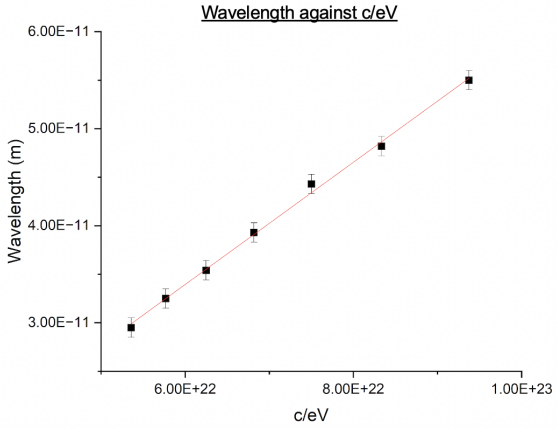

FIG. 14. A linear fit of the Daune-Hunt Law using values of $\lambda_{\min}$ recored from a diffraction pattern at a range of voltages.

Peak broadening

The first key observation was the broadening of intensity peaks, which were aligned nicely with Gaussian distributions. As mentioned, it was observed that the majority of peaks lined up with the distributions of a constant full width half maximum of $4\Delta\theta$ suggesting precision error and hence presenting a limitation of the apparatus. However, taking a qualitative visual analysis of FIG. 6 it is clear that this is not always the case. Along with that, if peak broadening was entirely dependant on the angle precision $\Delta\theta$ we'd expect an average FHWM of $2\Delta\theta$. Therefore peak broadening must have an additional source. It is in-fact known that peak broadening is a result of defects within our sample, or rather its microstructure [6]. Thus, both the sample imperfections and the precision of the apparatus contribute towards peak broadening. A possible route of further investigation would be to quantify these contributions via the assumption that our final Gaussian shaped peak is a convolution of two Gaussians, where final

width would be given by:

$$W_{final} = \sqrt{W_{exp}^2 + W_{def}^2}$$

Lattice structures and peak displacement

The literature values of lattice constant a for NaCl and Si are $a_{\text{NaCl}} = 2.814\mathring{A}$ and $a_{\text{Si}} = 5.43\mathring{A}$ [1] respectively. Looking back at the measured values of d and applying equation 2 it is clear that for NaCl; $\sqrt{h^2 + k^2 + l^2} = 1$, this aligns with the theory that NaCl is a cubic lattice structure and has a crystal plane with miller indices (100). Similarly, using the theory that Silcion is a diamond crystal structure where diffraction occurs on the plane (111) followed by the application of equation 2 we find a measured lattice constant of 5.425 ± 0.009Å. The experimental value of a_{NaCl} is 99.3% accurate and a_{Si} is 99.9% accurate - initially surprising since the theoretical and experimental patterns in both FIG. 7 and 8 are noticeably different. The most important result here is that the 'shift' spans across the entire diffraction pattern, suggesting the cause remains constant throughout measurements, therefore disregarding any factors that could vary. A likely cause is simply the misplacement of the sample itself along with the mis-alignment of the equipment. Applying the shift to Braggs law gives:

$$n\lambda = 2d\sin(\theta + \theta_s)$$

Following this logic it can be shown that although 0.3° and 0.45° seems large when taken through the sine and cosine functions the change is minimal:

$$\sin(\theta + \theta_s) = \sin(\theta)\cos(\theta_s) + \cos(\theta)\sin(\theta_s)$$

$$\cos 0.3 \approx \cos 0.45 \approx 1$$

$$\sin 0.3 \approx \sin 0.45 \approx 0$$

and so:

$$2d\sin(\theta + \theta_s) \approx 2d\sin\theta$$

This explains why, regardless of the shift, the accuracy of the results is so close to perfect. However, using such logic we'd still expect NaCl (that has a smaller shift) to be more accurate. Why exactly this result was recorded may relate to the way d was calculated. d was determined by the gradient of a linear fit of Bragg's Law. Since Si $n = 2$ peaks are not observed (FIG. 8), results span across both a larger angle range $(5^\circ < \theta_i < 27^\circ)$ and a larger n range $(n = 1, 3, 4)$ than NaCl ($6^\circ < \theta_i < 22^\circ$, $n = 1, 2, 3$). Consequently, the Si linear fit is more accurate.

Absorption edge analysis

The value of Rydberg constant recorded via presented analytical methods was the least accurate result throughout the paper, being only 81% accurate relative to the literature value of $10,973,731.6\text{m}^{-1}$. Once again, with a quick glance at FIG. 10, given the noise observed it may be assumed that the apparatus is causing broader, 'slanted' edges. However, this is not entirely the case. A key theory is missing; Heisenberg's uncertainty principle. Returning to the theory of absorption, a repercussion of the ionization of electrons is the opening of a vacancy within it's corresponding energy level [3]. This is an unstable state until this vacancy is filled. The lifetime of such vacancy is given by Δt and must abide by the heisenberg principle [7]:

$$\Delta t \Delta E \geq \frac{\hbar}{2}$$

Where ΔE is the uncertainty on x-ray energy. Since lifetime Δt is likely very small, ΔE must be relatively large. Such effects on either side of an absorption edge broaden out the edge to produce an 'arc-tangent shaped' edge as observed. Hence, this uncertainty is why the slope of each edge is slightly different.

With this theory in mind there is still room for improvement. The most obvious method to improve the value of Rydberg constant would be to use additional elements. In this case, the small sample size of 5 materials is a clear limiting factor.

Planks Constant

There is little to discuss in regards to the measurements λ_{min} and determination of Planck's constant. The result obtained is 95.4% accurate, with it's upper bound being 97.5% accurate. Why the correct result is not encapsulated within the these bounds is unknown and in this case could solely be due to precision error of the apparatus which was not correctly accounted for. However, this can not be concluded and would require repeat experiments. Nevertheless, this level of accuracy is impressive.

Areas of Further Investigation / Bremmstraulung

The final undiscussed result is that shown in FIG. 9. The plot labeled initial is the an exact plot of Kramers' law (8) using the parameters I_{max} and λ_{min} from the experimental result. Although this plot follows the same general shape as the observed pattern, it is considerably different. The second plot, labelled 'altered' follows a tweaked version of Kramer's law given by :

$$I(\lambda)d\lambda = K[\frac{\lambda - (\lambda_{\text{min}} - a)}{a}]\frac{1}{[\lambda - (\lambda_{\text{min}} - a)]^2}d\lambda$$

and K is now given by;

$$4a^2 I_{\text{max}}$$

where a is a constant. In FIG. 9 the 'altered plot' was found with trial and error. Changing a over a range of values, it was found that the best value of a to fit the NaCl diffraction pattern was 11pm (to 1.d.p) or $0.37\lambda_{\text{min}}$. Even so, this altered pattern still does not drop in intensity as quickly as the measured pattern. Why exactly these observations are made is a topic that also requires the collection of more data and additional investigation.

CONCLUSIONS

In conclusion, it is clear that the Leybold x-ray is exceptionally accurate. Although initially recorded diffraction and absorption patterns appear somewhat far from what original theory predicts, it is only due to limited understanding. In the cases discussed it is often the effects of quantum mechanics that are not accounted for. Both aims - showing how much information a diffraction pattern contains, and analysing the apparatus' accuracy - were fulfilled.

REFERENCES

[1] Kittel C., Introduction to solid state physics. Crystal Structure, pp.3-26

[2] P. P. Ewald, 50 Years of X-ray Diffraction, William Henry Bragg, pp.315-317

[3] Shankland, R. S. (1960) Atomic and nuclear physics. 2d edn. New York: Macmillan. X-rays, pp. 174-229

[4] Cowley, J. M. and Cowley, J. M. (1992) Electron diffraction techniques. pp. 1-5

[5] Laguitton, Daniel; William Parrish (1977). "Experimental Spectral Distribution versus Kramers' Law for Quantitative X-ray Fluorescence by the Fundamental Parameters Method". X-Ray Spectrometry

[6] Rajeswari Yogamalar, Ramasamy Srinivasan, Ajayan Vinu, Katsuhiko Ariga, Arumugam Chandra Bose, X-ray peak broadening analysis in ZnO nanoparticles,Solid State Communications, Volume 149, 2009.

[7] Sen, D. (2014). "The Uncertainty relations in quantum mechanics" (PDF). Current Science. 107 (2): 203–218